Research article

MISSENSE MUTATIONS IN *IHH* IMPAIR INDIAN HEDGEHOG SIGNALING IN C3H10T1/2 CELLS: IMPLICATIONS FOR BRACHYDACTYLY TYPE A1, AND NEW TARGETS FOR HEDGEHOG SIGNALING

SHENGZHEN GUO[1,2,3§], JIAN ZHOU[1,2§], BO GAO[1,2,3], JIANXIN HU[1,2,3], HONGSHENG WANG[1,2], JUNWEI MENG[1,2], XINZHI ZHAO[1,2], GANG MA[1,2], CHUWEN LIN[1,2], YUE XIAO[1,2], WEI TANG[1,2], XUMING ZHU[1,2], KATHRYN S.E. CHEAH[3], GUOYING FENG[4], DANNY CHAN[3]*and LIN HE[1,2,5]*
[1]Institute for Nutritional Sciences, Shanghai Institutes for Biological Sciences, Chinese Academy of Sciences, Shanghai 200031, China, [2]Bio-X Center, Key Laboratory for the Genetics of Developmental and Neuropsychiatric Disorders (Ministry of Education), Shanghai Jiao Tong University, Shanghai 200030, China, [3]Department of Biochemistry, The University of Hong Kong, Pokfulam, Hong Kong, China, [4]Shanghai Institutes of Mental Health, Shanghai 200030, China, [5]Institutes of Biomedical Sciences, Fudan University, Ming De Building, 138 Yi Xue Yuan Road, Shanghai 200032, PR China

Abstract: Heterozygous missense mutations in *IHH* result in Brachydactyly type A1 (BDA1; OMIM 112500), a condition characterized by the shortening of digits due to hypoplasia/aplasia of the middle phalanx. Indian Hedgehog signaling regulates the proliferation and differentiation of chondrocytes and is essential for endochondral bone formation. Analyses of activated IHH signaling in C3H10T1/2 cells showed that three BDA1-associated mutations (p.E95K, p.D100E and p.E131K) severely impaired the induction of targets such as *Ptch1*

§These authors contributed equally to this work

* Authors for correspondence: Dr. Lin He, Bio-X Center, Shanghai Jiao Tong University, Cental Little White House, 1954 Huashan Road, Shanghai 200030, China, tel./fax: 86-21-62822491, e-mail: helin@bio-x.cn and Dr. Danny Chan, Department of Biochemistry, The University of Hong Kong, 3/F, Laboratory Block, Faculty of Medicine Building, 21 Sassoon Road, Pokfulam, Hong Kong, China, tel.: 852-28199482, fax: 852-28551254, e-mail: chand@hkusua.hku.hk

and *Gli1*. However, this was not a complete loss of function, suggesting that these mutations may affect the interaction with the receptor PTCH1 or its partners, with an impact on the induction potency. From comparative microarray expression analyses and quantitative real-time PCR, we identified three additional targets, *Sostdc1*, *Penk1* and *Igfbp5*, which were also severely affected. *Penk1* and *Igfbp5* were confirmed to be regulated by GLI1, while the induction of *Sostdc1* by IHH is independent of GLI1. SOSTDC1 is a BMP antagonist, and altered BMP signaling is known to affect digit formation. The role of *Penk1* and *Igfbp5* in skeletogenesis is not known. However, we have shown that both *Penk1* and *Igfbp5* are expressed in the interzone region of the developing joint of mouse digits, providing another link for a role for IHH signaling in the formation of the distal digits.

Key words: Indian Hedgehog, Brachydactyly type A1, Microarray, EMSA

INTRODUCTION

The Hedgehog gene (*Hh*) was initially identified in *Drosophila* as a segment polarity gene [1]. In mammals, the Hedgehog family includes the *Sonic* (*Shh*), *Indian* (*Ihh*) and *Desert* (*Dhh*) *hedgehog* genes. They represent key signaling molecules that mediate fundamental developmental processes, controlling the growth, patterning and morphogenesis of many regions of the body plan. SHH has been implicated in establishing the early left-right axis [2, 3] and the anterior and posterior axis in the limbs [3], and in regulating ventral cell fates in the central nervous system [4]. DHH has roles in germ-cell proliferation towards the late stages of spermatogenesis, in sertoli cell signaling, and in peripheral nerve ensheathment [5]. IHH has key roles in chondrogenesis, regulating the proliferation and differentiation of chondrocytes [6].

So far, studies have suggested that the Hedgehog genes signal through a similar mechanism controlled by two transmembrane proteins, SMO and PTCH. Genetic and biochemical studies have shown that PTCH suppresses the constitutive activity of SMO, and that the binding of Hedgehog to PTCH relieves this suppression, allowing the activation of downstream targets such as *Ptch1* and *Gli1*, through the Ci/GLI family of transcriptional effectors [7-9]. It is not known how SHH, IHH and DHH control distinct biological processes during

development. IHH has similar biological properties to those of SHH, including the ability to regulate the conserved target genes, such as *Ptch1* and *Gli1* [6-9]. Other activated genes include the bone morphogenetic proteins, such as *Bmp2* and the 5' Hoxd gene cluster (*Hoxd11*, *12* and *13*) [3, 10, 11]. IHH is best known for its role in endochondral ossification, where it has a direct role in regulating chondrocyte proliferation, and where, via parathyroid hormone-related protein (PTHrP), it regulates chondrocyte hypertrophy through a negative feedback mechanism [6, 12]. *Ihh* is initially expressed in the chondrocytes of the early cartilaginous skeletal elements. On maturation, its expression becomes progressively restricted to post-mitotic prehypertrophic chondrocytes [13]. Its importance in endochondral ossification is highlighted in *Ihh*-null mouse mutants (*Ihh$^{-/-}$*), which exhibit a severe reduction in skeletal growth [14]. Recently, we and others have shown that heterozygous missense mutations in *IHH* are associated with Brachydactyly type A1 (BDA1), an autosomal dominant disorder characterized by shortened or missing middle phalanges [reviewed in 15 and 16].

Interestingly, the first three mutations that we identified – c.G283A (p.E95K), c.G391A (p.D100E) and c.C300A (p.E131K) – cluster on conserved amino acids across known vertebrate and invertebrate Hedgehog proteins, suggesting that these amino acids are important for Hedgehog function. Furthermore, they lie in close proximity on the surface of a groove for a molecular structure of IHH modeled on the X-ray crystal coordinates of SHH [17]. We hypothesize that these mutations affect IHH signaling through impaired interaction with interacting partners such as patched (PTCH), dispatched (DISP) and Hedgehog interacting protein 1 (HIP1). This hypothesis is supported by structural and biophysical analyses of IHH and its associated human mutations that cause BDA1, showing impaired interaction with its partners, such as PTCH1, HIP1 and CDO [18]. Furthermore, from the study of a mouse model for BDA1 carrying the p.E95K mutation, it was shown that this mutation not only affected the IHH signaling capacity, but also its range, which may be regulated by its interaction with PTCH1 and HIP1; thus, the mutant IHH signals outside its normal range, disrupting distal digit formation [19].

We aimed to gain further mechanistic insights into the *IHH* mutations causing BDA1 by studying the downstream consequence of these mutations on the expression of genes regulated by HH signaling. Here, we present evidence that the Hedgehog signaling was impaired in the three *IHH* mutations studied. In a comparative microarray analysis of gene expression profiles for genes that are not up-regulated relative to wild type IHH, *Sostdc1*, *Penk1* and *Igfbp5* were identified as possible new IHH signaling targets that may contribute to the molecular mechanism for BDA1. We confirmed that *Penk1* and *Igfbp5* are expressed in the developing joints of the distal digits in the mouse, and are activated via the transcription factor, GLI1.

MATERIALS AND METHODS

Expression and purification of recombinant IHH-N proteins

A cDNA encoding the amino-terminal domain of human IHH (amino acid residues 28-202) was amplified from an adult liver cDNA library, and the p.E95K (M1), p.E131K (M2) and p.D100E (M3) mutations were introduced by PCR mutagenesis using the respective primers: 5'-CTTCAAGGACGAG**A**AGAACACAGGCG-3'; 5'-GCTGCGGGTGACC**A**AGGGCTGGGACG-3', and 5'-CACAGGCGCCGA**A**CGCCTCATGACCC-3'.

The bolded and underlined nucleotides represent the single nucleotide substitution in each of the primers. The amplified regions were verified by DNA sequencing and cloned into the pGEX-2T expression vector (Amersham) as GST-fusion constructs with a thrombin cleavage site in between. IHH-N proteins were expressed in *E. coli* BL21 (DE3) and purified using a previously described method [20]. The purity and identity of the IHH-N proteins were assessed by SDS-PAGE and by western-blot analysis with an IHH antibody (SC-1782, SantaCruz).

Induction of Hedgehog signaling in C3H10T1/2 cells using purified IHH-N proteins

C3H10T1/2 cells (ATCC) were cultured in BME supplemented with 10% FBS, 100 U/ml penicillin and 100 μg/ml streptomycin, at 37ºC in a humidified incubator containing 5% CO_2. To assess the induction of Hedgehog signaling for the wild type (Wt) and mutant IHH-N proteins, C3H10T1/2 cells grown to confluence in 12-well plates were cultured for 5 days in the presence of IHH-N proteins at different concentrations as indicated in the Results section. All of the induction assays were performed in triplicate.

Induction of Hedgehog signaling in transiently transfected C3H10T1/2 cells

Full-length human *IHH* cDNA expression constructs were generated and cloned into the pCMV-TnT vector (Promega). The vectors used in these experiments included pCMV-Wt-*IHH* (Wt-*IHH*), pCMV-M1-*IHH* (p.E95K mutation), pCMV-M2-*IHH* (p.E131K mutation), pCMV-M3-*IHH* (p.D100E mutation), with the empty vector as a control.

One day before the transfection, C3H10T1/2 cells were plated at a density of $2x10^5/cm^2$ in 24-well plates and cultured in BME supplemented with 10% FBS in the absence of an antibiotic. This allowed the cells to reach 80-90% confluency before transfection with 0.7 μg of plasmid DNA per well using LipofectamineTM 2000 (Invitrogen) according to manufacturer protocol #11668. All of the transfection experiments were performed in triplicate. The expression of the IHH proteins was also verified by western-blot using an SHH antibody (SC-9024, Santa Cruz) that cross-reacts with IHH.

A GLI1 induction assay was used to study specific downstream targets of GLI1 in the transfected C3H10T1/2 cells. A plasmid vector, pCMV-Flag-m*Gli1* (a full-length mouse *Gli1* cDNA construct) was used to express GLI1 in C3H10T1/2

cells, and an empty pCMV-TnT vector was used as a control. The Flag-m*Gli1* cDNA plasmid was donated by Dr. Alexandra L. Joyner (NYU Medical Center).

Microarray analysis of IHH targets in C3H10T1/2 cells
Total RNA was isolated from C3H10T1/2 cells using the Trizol reagent (Invitrogen). Biotin-labeled cRNA probes were generated from total RNA using the Enzo RNA Transcript Labeling Kit (Affymetrix), further purified using the RNeasy Mini Kit (Qiagen), and fragmented in a fragmentation buffer (40 mM Tris-acetate, pH 8.1, 100 mM potassium acetate, and 30 mM magnesium acetate). 20 μg of labelled-cRNA was applied to each array. The cRNA yield did not differ significantly between the different samples, and the quality of the RNA samples was initially verified by test-array hybridization.

The array analysis was performed by the GeneTech Biotechnology Company Limited (Shanghai, China) using mouse GeneChips 430A (Affymetrix, Santa Clara, CA). The sample labelling, hybridizaiton and scanning procedures were as described in the Affymetrix GeneChip Expression Analysis Technical Manual.

The data analysis was carried out on five chips, corresponding to the control (un-induced cells), and cells induced with the Wt, M1, M2 and M3 IHH-N proteins. The Mouse 430A chip contains 18,000 genes and each gene is represented by 11 pairs of oligoucleotide probes. Each probe pair is 25-mer in length and is either a perfect match or a single central mismatch. The hybridization intensities were expressed as an average difference (subtracting the intensity of the mismatch probes from the intensity of the perfect match probes). The average difference values from the mouse GeneChip analysis were exported into the Excel program and then converted to ratios of fold-expression over background; that is, the fold difference between un-induced C3H10T1/2 cells relative to cells induced with the Wt or mutant M1, M2 and M3 IHH-N proteins. The fold-expression ratios were sorted using Microssoft Excel. To identify the common genes that are similarly altered between the Wt and the mutant group, we only considered genes with changes in the fold-expression ratios > 1.6 in the mutant groups when compared to the Wt group. These genes were then selected for verification by quantitative real-time PCR.

RNA preparation and quantitative real-time PCR
Total RNA was isolated from C3H10T1/2 cells using Trizol reagent (Invitrogen) as described above, and oligo *d(T)*-primed cDNA was prepared from 1 μg RNA using the SuperScript First-Strand Synthesis System for RT-PCR (Invitrogen). The targeted genes were amplified and quantified using SYBR Green I fluorescence in quantitative real-time PCR as previously described [21]. The primers for the quantitative real-time PCR of the respective genes are listed in Tab. 1. Three separate PCR reactions were performed for each sample on an ABI PRISM 7900 Detection System (Applied Biosystems). In brief, each reaction was performed in a total volume of 10 μl containing 10 ng of cDNA

(10 ng), 5 µl Taqman® Universal PCR Master Mix (Applied Biosystems), 500 nM of each primer and $0.2 \times$ SYBR® Green I (Molecular Probe, Inc.). All of the gene signals were normalized to the *Gapdh* signal.

Tab. 1. The primers for quantitative real-time PCR

Gene	Product lengt	Primers (5'-3')
Gapdh	107 bp	GAAACCTGCCAAGTATGATGACA GGTCCTCAGTGTAGCCCAAGA
Ptc1	82 bp	TCAGTTGACTAAACAGCGTCTGGTA GACCCAAGCGGTCAGGTAGAT
Gli1	95 bp	GGCTGTCGGAAGTCCTATTCAC CAACCTTCTTGCTCACACATGTAAG
Pthrp	78 bp	GGAGATCCACACAGCCGAAA TGGTTTTTGGTGTTGGGAGC
Akp2	78 bp	GCCTGGATCTCATCAGTATTTGG GTTCAGTGCGGTTCCAGACAT
Col2a1	78 bp	GAGCAGCAAGAGCAAGGAAAA TCGCCATAGCTGAAGTGGAA
Sostdc1	89 bp	AGTTTGCAGTGAAAGCCAGGC ACAGAATGCAGCATCAGGTGC
Penk1	71 bp	AATTTCCTGGCGTGCACACT TCCTTGCAGGTCTCCCAGAT
Igfbp5	71 bp	TGTGTGGACAAGTACGGAATGAA AAGGCGTGGCACTGAAAGTC

The GenBank accession numbers of the genes above are listed sequentially as follows: BC083080, U46155, AB025922, BC058187, J02980, BC030913, AY255635, BC049766, L12477.

Whole cell extracts containing GLI1 proteins

Cell extracts containing GLI1 proteins (GLI1 cell extract) were prepared from CHO cells transfected with the pCMV-Flag-m*Gli1* plasmid, with untransfected cells as the control. Cell pellets were lysed in ice for 30 min using the Totex buffer (20 mM HEPES, pH 7.9, 350 mM NaCl, 1% NP-40, 20% Glycerol, 0.5 mM EDTA, 0.1 mM EGTA, 1 mM $MgCl_2$, 1 mM PMSF, 1 mM DTT) containing a complete protease inhibitor cocktail (Roche). Cell debris was removed by centrifugation at 12,000 x g, 4ºC for 20 min. The presence of the Flag-tagged GLI1 proteins in the Gli1 extract was confirmed by western-blot analysis using a Flag-M2 antibody (Stratagene).

Electrophoresis mobility shift assay (EMSA)

EMSA assays were carried out in a final volume of 20 µl containing 20 mM HEPES, pH 7.9, 2 mM $MgCl_2$, 2 mM DTT, 0.5 mM EDTA, 10% Glycerol, 0.5 mg/ml BSA and 0.05 mg/ml Poly dI-dC. Each reaction contains 1 µl (35 fmol) of 29-bp double-stranded ^{32}P-labeled probes with approximately 6-10 µg GLI1

or control cell extracts, and when appropriate, 2 μl (1.75 pmol) of matched unlabelled competitor oligonucleotides, or control competitor oligonucleotides with mismatches in the GLI-binding site. The binding reaction was carried out at RT for 30 min, and the resultant products were analyzed by polyacrylamide gel electrophoresis and the radioactive bands visualized on Kodak MIN-R2000 films. When performing super-shift, the proteins were pre-incubated with an appropriate antibody at RT for 1 h prior to the addition of the probe.

In situ hybridizations

An *Igfbp5* probe (1174 bp) was generated by PCR amplication from cDNA prepared from C3H10T1/2 cells using the primers 5'-GCCTCTCGGGTCTGT-CCCCT-3' and 5'-TTACCCACCATCTGGGCCCT-3', cloned into the pGEM-T vector (Promega), and verified by sequencing. The *Penk1* probe (430 bp) was donated by Dr Sarah Herzog, Max-Planck-Institute of Experimental Endocrinology. The sense and antisense probes were labelled with DIG using standard protocols with SP6 or T7 polymerase (Roche). The *Ihh*-null heterozygous mutant mouse was donated by Dr Andrew P. McMahon [14]. For the whole mount *in situ* hybridization, the limbs from the mouse embryos at E13.5 and E14.5 were fixed at 4ºC in 4% paraformaldehyde overnight, and hybridization with the sense and antisense probes was performed as described previously [22]. Color development was done with BM purple AP substrate (Roche) at 4ºC overnight.

RESULTS

Establishing a cell-culture system for the analysis of IHH signaling

C3H10T1/2 is a well-established reporter cell line for Hedgehog signaling for SHH-N [23] and IHH-N proteins [24, 25], with the signal transduced through the PTCH/SMO/GLI pathway. We tested C3H10T1/2 cells for suitability as an assay system for detecting differences in response to Wt and mutant IHHs. C3H10T1/2 cells were transfected with an expression vector for the full-length Wt *IHH* cDNA. The induction of the known target genes *Ptch1* and *Gli1* was measured by quantitative real-time PCR over a period of 5 days. As expected, both of these targets were activated within the first day after transfection, and were maintained over the 5-day period with the maximum on day 2 (Fig. 1). On day 2, *Ptch1* and *Gli1* had been respectively induced by 15- and 58-fold in Wt *IHH* transfected cells relative to control cells transfected with an empty vector. However, an indirect target of IHH, *Pthrp*, had not been induced. On the other hand, *Col2a1*, a marker for chondrogenesis, had been slightly induced relative to the control, also with a maximal level of 3-fold on day 2 (Fig. 1). Alkaline phosphatase 2 (*Akp2*), a marker for osteogenesis, was induced from day 2, and reached a maximal level of 9-fold on day 4 (Fig. 1).

The differentiation progression of C3H10T1/2 cells to osteoblasts upon Hedgehog signaling is well documented [23, 24], and can be used as an indicator

of Hedgehog signals. From this analysis, it appears that day 5 may be most informative for the measurement of the transcription activation of *Ptch1* and *Gli1*, as well as the progression to osteogenesis based on *Akp2* gene expression.
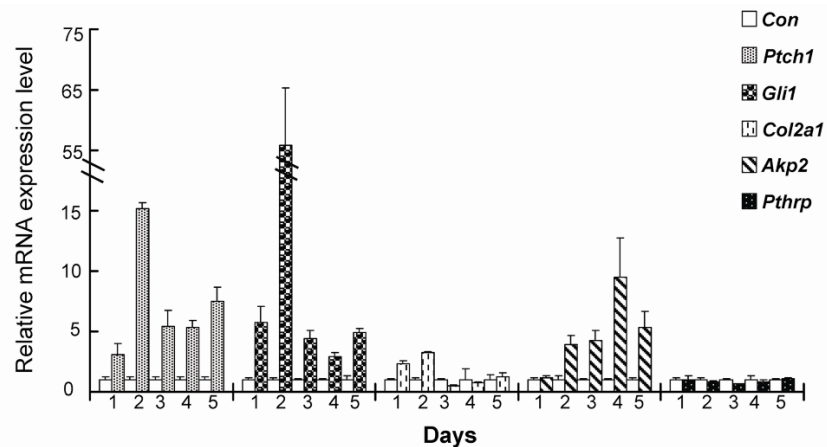

Fig. 1. The optimal *in vitro* conditions for the analysis of IHH signaling in C3H10T1/2 cells. C3H10T1/2 cells were cultured over a period of 5 days transfected with full-length Wt *IHH* cDNA in 24-well plates. Total RNA was extracted from cells harvested daily, and the relative expression levels of the indicated genes were assessed by quantitative real-time PCR. The expression levels of all of the genes tested were normalized to the *Gapdh* mRNA level in each sample. The relative mRNA expression (y-axis) represents the fold change for the expression of the genes relative to control cells that were not supplemented with Wt IHH-N. Each data point represents the mean with the standard deviation of tree separate experiments, each performed in triplicate.

Hedgehog signaling was severely impaired for IHHs with BDA1 mutations
As expression levels in transfected cells are difficult to control precisely, we performed a quantitative induction analysis of *Ptch1*, *Gli1* and *Akp2* using purified IHH-N (the N-terminal functional portion of Hedgehog proteins). We tested various concentrations of the Wt IHH-N protein at concentrations from 0 to 1000 nM, and found that 500 nM to 750 nM was the optimal concentration range on day 5 of induction (data not shown). We compared the induction activity of the three BDA1 mutant IHH-N proteins, p.E95K (M1), p.E131K (M2) and p.D100E (M3), with Wt IHH-N at 500 nM in C3H10T1/2 cells. Wt IHH-N induced expression of *Ptch1*, *Gli1* and *Akp2,* when compared with the uninduced control cells (Fig. 2A). By contrast, none of the mutant IHH-N (M1, M2 and M3) proteins induced *Ptch1* expression to any significant level, while *Gli1* was mildly induced, but to levels significantly lower than those induced by Wt IHH-N (Fig. 2A). The *Akp2* expression remained at basal levels for all of the mutant IHH-N proteins, compared to a 2.4-fold increase for Wt IHH-N (Fig. 2A). Furthermore, the Wt and mutant IHH-N proteins were stable throughout the 5 days of the incubation period (data not shown),

indicating that the observed impaired activation of Hedgehog signals for the mutant IHH-N proteins was not due to a preferential degradation.
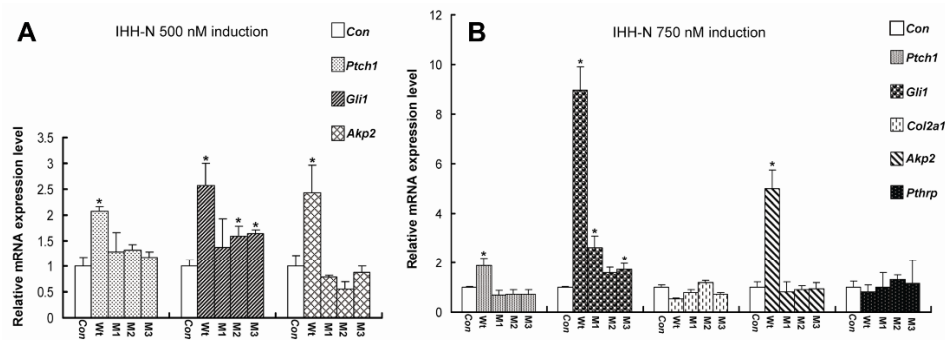

Fig. 2. The relative potency of Wt and mutant IHH-N signaling in C3H10T1/2 cells. C3H10T1/2 cells were cultured for 5 days in 12-well plates supplemented with 500 nM (A) or 750 nM (B) of Wt and mutant (M1, M2 and M3) IHH-N proteins. At the end of the 5-day period, the total RNA was extracted from the cells, and the relative expression levels of the genes indicated were assessed by quantitative real-time PCR. Bars with an asterisk indicate genes with a statistically significant induction level relative to the control cells, with $p < 0.015$. In all of the experiments, the normalization and standard deviation calculations were performed as described in Fig. 1. Wt: wild type, M1: p.E95K mutation, M2: p.E131K mutation, and M3: p.D100E mutation.

An additional induction experiment with Wt IHH-N showed that the optimal induction concentration was closer to 750 nM. Therefore, we repeated the Hedgehog signaling induction comparison between the Wt and mutant IHH-N proteins at 750 nM, and also included an induction expression analysis of *Col2a1* and *Pthrp*. A similar pattern of induction to the 500 nM concentration was obtained for *Ptch1*, *Gli1* and *Akp2* (Fig. 2B), again with a significant induction impairment for the mutant IHH-N proteins compared with the Wt. Consistent with the cell transfection study (Fig. 1), neither *Col2a1* nor *Pthrp* were induced by the mutant and Wt IHH-N proteins (Fig. 2B). Interestingly, while the induction of *Gli1* was relatively higher at 750 nM (9-fold) compared to 500 nM (2.5-fold) for the Wt IHH-N, the induction of *Ptch1* remained similar (2-fold), indicating that the level of *Gli1* induction by IHH is more sensitive to the HH concentration than *Ptch1*. Like *Gli1*, the induction of *Akp2* was similarly elevated to 5-fold at 750 nM compared to 2.5-fold at 500 nM for the Wt IHH-N. The *Akp2* expression remained at basal levels for all of the mutant IHH-N proteins.

Mature Hedgehog proteins are modified by two lipid groups, an N-linked palmitate at the amino terminus, and a covalently bound cholesterol at the C-terminus [25]. These modifications are not present when the IHH-N proteins are expressed and purified from *E. coli,* but can significantly enhance *in vitro* Hedgehog signaling [26]. Therefore, we performed transfection expressions in the C3H10T1/2 cells with Wt and mutant full-length cDNA constructs for

a comparison of *Ptch1* and *Gli1* induction. IHH expressed in a mammalian cell system would be fully processed and modified, allowing optimal activity. Although semi-quantitative, the expression level and presumably the transfection efficiency were similar for the Wt and mutant constructs when the IHH protein level from the cell extracts was assessed by western-blot analysis (Fig. 3A).
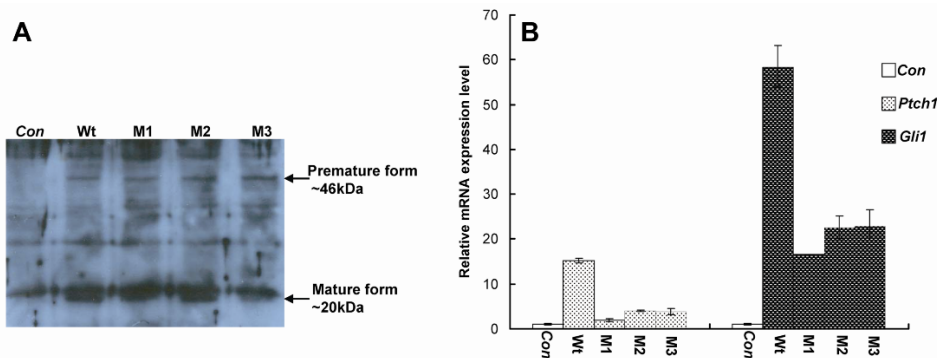

Fig. 3. The relative potency of Wt and mutant *IHH* cDNA signaling in C3H10T1/2 cells. C3H10T1/2 cells were transfected with a control vector or vectors carrying Wt or mutant *IHH* cDNA. A – IHH protein expression from the cell extract was verified by western-blot analysis. The precursor form of IHH is around 46 kDa and the active form is around 20 kDa, as indicated by the arrows. B – The total RNA was extracted 24 after transfection, and the relative expression levels of the genes indicated were assessed by quantitative real-time PCR. The control represents cells transfected with an empty vector. In all of the experiments, the normalization and standard deviation calculations were performed as described in Fig. 1.

Given that 2 days following the transfection was the optimal induction period for the Wt *IHH* (Fig. 1), we performed a quantitative real-time PCR analysis of *Ptch1* and *Gli1* induction comparing the cells' transfected Wt and mutant *IHH* cDNA constructs 2 days after transfection. Consistent with the use of purified IHH proteins, the inductions of *Ptch1* and *Gli1* were significantly impaired for cells transfected with the mutant constructs, with a reduction of almost 70% compared to the Wt for *Gli1*, and one of 80% for *Ptch1* (Fig. 3B). The difference in the *Akp2* expression between the Wt and mutant IHH-N was reflected in a reduced enzymatic activity, confirmed using an alkaline phosphatase staining assay of the C3H10T1/2 cells after 5 days of induction (data not shown).

Together, the cell transfection and protein induction data suggested that the mutations p.E95K, p.E131K and p.D100E in *IHH* impaired the transduction of Hedgehog signals, but did not cause a complete loss of function. While the *in vitro* conditions used here may not be a true reflection of the physiological concentrations, the data nevertheless supports a significant difference between the Wt and mutant IHH proteins and is consistent with the recent reports on the impact of such mutations [18, 19].

Identification of genes that were differentially induced in Wt and mutant IHH signaling

The differential induction of the Hedgehog target genes (*Ptch1* and *Gli1*) between the Wt and mutant IHH proteins offered an opportunity to perform a comparison of gene expression profiles to identify additional Hedgehog targets that may be similarly affected. A comparative microarray expression analysis was performed using the Mouse 430A chip from Affymetrix for RNAs extracted from C3H10T1/2 cells transduced for 5 days with 750 nM of Wt and mutant IHH-N proteins and for RNAs from uninduced cells.

Tab. 2 summarizes the number of genes identified in each array and the differences in the comparative analysis. To identify the genes that are affected, we focused on the genes that are at least 1.6-fold down-regulated in the mutant IHH-N-induced cells relative to Wt. We then selected the genes in this list that are common in all the three mutant IHH-N-transduced cells. Five genes survived this filter: *Ptch1*, *Sostdc1*, *Igfbp5*, *Penk1* and *Rbbp4*. The inclusion of *Ptch1* in this small list of genes suggested that the filtering process is reasonable, and sufficiently stringent to identify known targets. Surprisingly, *Gli1* was not included in this list. On closer inspection, it appeared that *Gli1* was not well detected in the Wt and mutant IHH-N inductions, which may be ascribed to a low probe specificity and efficiency for this gene in the Affymatrix Mouse 430A chip.

Tab. 2. A summary of the gene numbers in the comparative gene expression profiling

Array[a]	No. of genes determined to be expressed[b]	Comparisons	No. of genes with an increase $\geq$ 1.6-fold[c]	No. of genes with a decrease $\geq$ 1.6-fold[c]
C	9919			
Wt	11263	Wt *vs* C	175	44
M1	10442	Wt *vs* M1	94	78
M2	11231	Wt *vs* M2	102	74
M3	11420	Wt *vs* M3	180	213

[a]Array hybridized with cRNA synthesized from total RNA extracted from the control (C) or 750 nM protein induction (Wt or mutant IHH-N , M1, M2 and M3). [b]If a gene transcript is determined to be expressed in the array, the detection scaling will be expressed as "Present" in the original data. [c]Fold changes of expression levels are expressed as the $\log_2$ ratio in the original data. A $\log_2$ ratio of 1 is the same as a Fold Change of 2.

Of the four genes that were identified as potential new targets of IHH signaling, only three, *Sostdc1*, *Igfbp5* and *Penk1*, were confirmed to be up-regulated in Wt IHH-N induction by quantitative real-time PCR (Fig. 4A). Among them, *Sostdc1*, encoding a secreted BMP antagonist [27], reached the highest induction level of 20-fold for the Wt proteins (Fig. 4A). We were unable to confirm any induction for *Rbbp4* (data not shown). However, the potential new IHH targets *Sostdc1*, *Igfbp5* and *Penk1* were not induced to any significant level by the mutant IHH-N proteins (Fig. 4A).
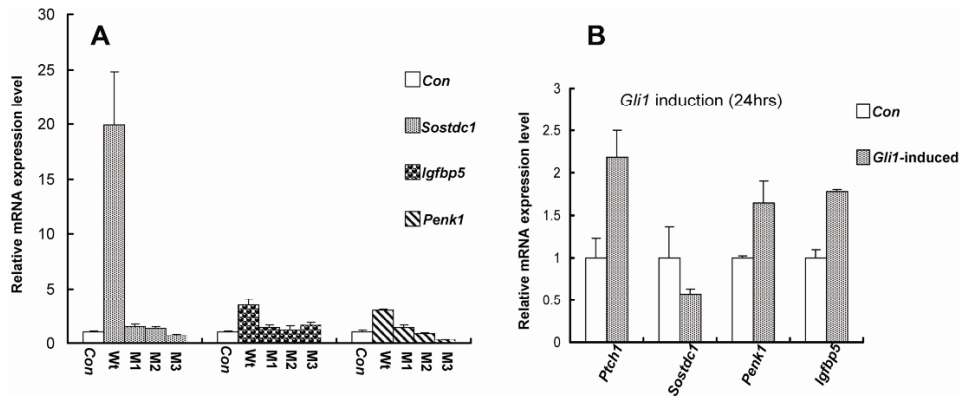
Fig. 4. Quantitative real-time PCR assessment of additional targets of IHH. A – C3H10T1/2 cells were cultured in 12-well plates for 5 days supplemented with 750 nM of Wt and mutant (M1, M2 and M3) IHH-N proteins. At the end of the 5-day period, the total RNA was extracted from the cells, and the relative expression levels of the new target genes *Sostdc1*, *Igfbp5* and *Penk1* were assessed by quantitative real-time PCR. B – C3H10T1/2 cells were transfected with a cDNA expression construct for the mouse *Gli1* gene. The total RNA was extracted 24 after transfection, and the relative expression levels of the genes indicated were assessed by quantitative real-time PCR. Genes with an asterisk indicate a statistically significant induction ($p < 0.020$) following *Gli1* transfection relative to the control cells transfected with an empty vector. The normalization and standard deviation calculations were performed as described in Fig. 1.

IHH signaling activates *Penk1* and *Igfbp5* via GLI1
At present, the known Hedgehog target genes are transduced/regulated by the GLI family of transcription factors (GLI1, GLI2 and GLI3) via the conserved HH-PTCH-GLI pathway [28, 29]. Therefore, we performed a transfection induction in C3H10T1/2 cells with a full-length mouse *Gli1* cDNA expression construct, and monitored the induction of *Sostdc1*, *Penk1* and *Igfbp5* by quantitative real-time PCR, with *Ptch1* expression as an internal positive control. As expected, 24 h after transfection with the *Gli1* cDNA construct, the mRNA level of *Ptch1* was up-regulated by a factor of 2.2-fold relative to the control cells (Fig. 4B). The expression levels of *Penk1* and *Igfbp5* were also significantly up-regulated upon *Gli1* transfection (Fig. 4B). Interestingly, the expression of *Sostdc1* was not up-regulated, but rather down-regulated upon *Gli1* transfection (Fig. 4B).
GLI1 is a sequence-specific DNA-binding protein that interacts with the motifs GACCACCCA, and the direct binding of GLI1 to this 9-bp consensus sequence in the *Ptch1* promoter was previously demonstrated in gel-shift assays [29, 30].
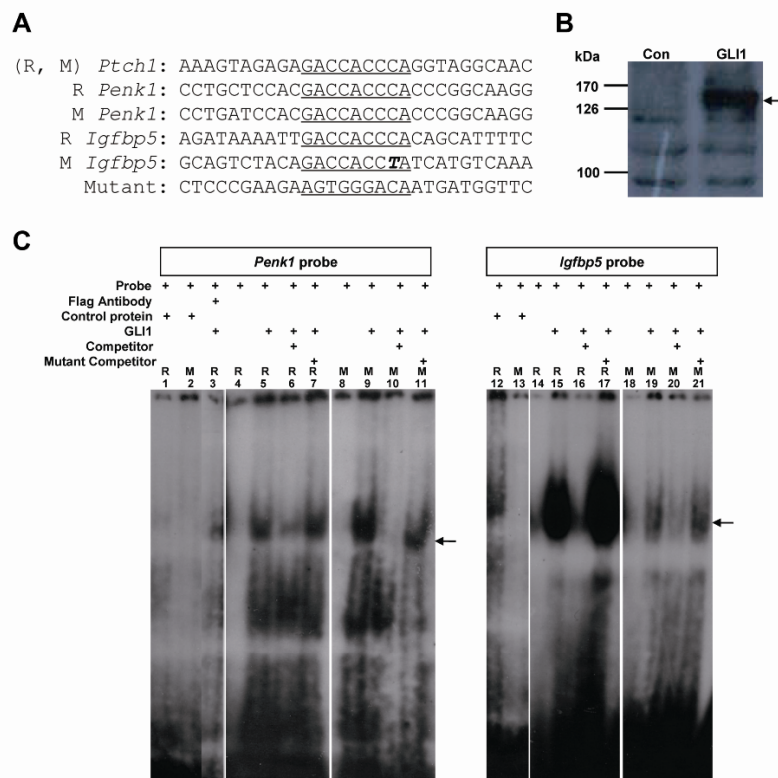
Fig. 5. Binding of GLI1 transcriptional factor to the promoter region of the newly revealed target genes. A – The sequences in the promoter regions of the mouse (M) and rat (R) *Ptc1*, *Penk1* and *Igfbp5* genes are sown with the putative GLI1-DNA binding motifs underlined. A base that differs from the conserved 9-bp consensus in the mouse *Igfbp5* is indicated in bold and italic. B – CHO cells were transfected with a mouse Flag-*Gli1* expression construct, and the presence of the GLI1 protein in the whole cell extracts (GLI1) verified by western-blot analysis using a Flag® antibody. A specific band (arrow) with an apparent MW of 120 kDa was detected specifically in the *Gli1*-transfected cells compared to the control CHO cells (Con). The whole cell extract containing GLI1 was used as the source of GLI1 proteins for EMSA. C – EMSA demonstrating the binding of GLI1 to DNA fragments containing putative GLI1 binding motifs identified in *Penk1* and *Igfbp5* (panel A). The sequences of the ^{32}P-labeled labelled probes are as indicated in panel A. The reagents present in each reaction are indicated with a plus sign (+). "GLI1" and "control proteins" respectively represent whole cell extracts from CHO cells transfected with a Gli1 expression vector or control CHO cells. The "competitor" is a 100-fold excess of unlabelled DNA probe, and the "mutant competitor" is a control competitor DNA with mismatches in the GLI-binding site (panel A). Products were analyzed by polyacrylamide gel electrophoresis and radioactive bands visualized on Kodak films. Super-sift was performed using a "Flag antibody" to the Flag-tagged GLI1 fusion protein. The arrow indicates the sifted bands. Lanes for the rat and mouse *Penk1* probes are as indicated in lanes 1-11, and the rat and mouse *Igfbp5* probes in lanes 12-21.

Given that the *Gli1*-transfection assay suggested *Penk1* and *Igfbp5* could be direct targets for GLI1, we evaluated these two genes in both the mouse and rat genomes, and identified the 9-bp consensus sequences in the core promoter regions of *Penk1* and *Igfbp5* (Fig. 5A). The putative 9-bp motifs are conserved in both mouse and rat *Penk1* and *Igfbp5,* with the exception of a one-base change in the mouse *Igfbp5* (Fig. 5A).

To directly demonstrate an interaction between GLI1 and the 9-bp motif in the promoter region of *Penk1* and *Igfbp5*, we performed electrophoretic mobility shift assays (EMSA) with GLI1 and DNA containing the consensus sequences in *Penk1* and *Igfbp5*. The source of the GLI1 proteins was from whole cell extracts of CHO cells transfected with a Flag-tagged *Gli1* cDNA expression construct. The presence of GLI1 proteins in the extract was confirmed by western-blot (Fig. 5B). The DNA fragments were generated from paired oligonucleotides representing a 29-bp region of the promoter containing the GLI1-binding motif (Fig. 5A). EMSA analysis clearly demonstrated the binding of GLI1 to DNA containing the 9-bp motif present in *Penk1* with the appearance of mobility shifted bands in the presence of cell extracts containing GLI1 (Fig. 5C, lanes 5, 7, 9 and 11). No mobility shifts were observed from the extract of the control CHO cells in the *Penk1*-GLI1 binding reactions (Fig. 5C, lanes 1 and 2). However, the Flag® antibody that would bind to the Flag-tagged GLI1 did not detect a supershift (Fig. 5C, lane 3). The reason for this is not clear, but it may be related to the binding of the GLI1 to the DNA masking the antibody epitope, or to the binding of the antibody to GLI1 interfering with its interaction with the DNA probe. Similar results were obtained for the binding of GLI1 to the motif in the promoter region of *Igfbp5* (Fig. 5C, lanes 12-21). The binding to DNA of the rat *Igfbp5* sequence was very strong (Fig. 5C, lanes 15 and 17) compared to the results for the mouse sequence (Fig. 5C, lanes 19 and 21). This may be the reason for the faint gel-shift band in the control reaction with cell extracts from the control CHO cells (Fig. 5C, lane 12).

Penk1 and *Igfbp5* are expressed at the interzone of a development joint in distal digit formation

To correlate IHH signaling with the possible involvement of the new targets, *Penk1* and *Igfbp5*, in the molecular consequence for BDA1, we performed whole-mount *in situ* hybridization to compare the expression pattern between Wt and *Ihh*-null (*Ihh*^{-/-}) mutant mouse digits. In the Wt digits, *Penk1* is expressed in the developing interzone, and *Igfbp5* expression is detected in the developing interzone, interdigital and phalangeal regions at E13.5 and E14.5 (Fig. 6). In *Ihh*^{-/-} mice, *Penk1* expression is abolished in the developing digits, and the expression of *Igfbp5*, although maintained in the interdigital and phalangeal regions, was not distinctly observed in the presumptive interzone (Fig. 6). These results suggest that in part, the expression of these two genes, in particular *Penk1*, in the developing digital joints is under the regulation of *Ihh* signaling.
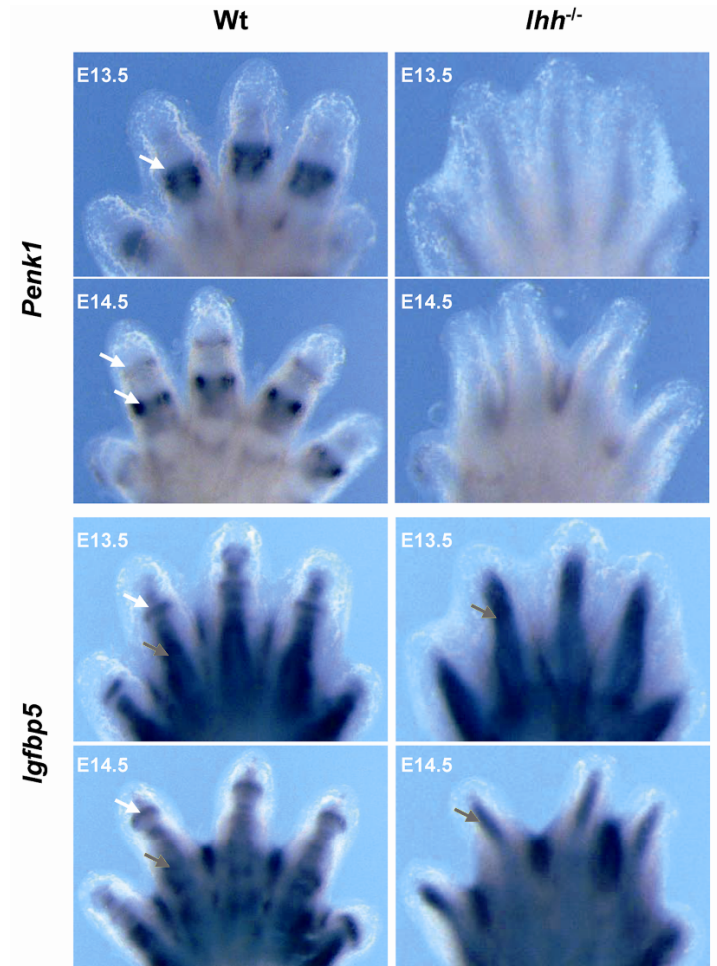
Fig. 6. The expression of *Penk1* and *Ifgbp5* in the mouse forelimb. A whole mount *in situ* hybridization of the forelimb sows the expression of *Penk1* and *Igfbp5* at E13.5 and E14.5. The white arrows indicate the position of the future phalangeal joint and the grey arrows indicate the position of phalangeal region.

DISCUSSION

Brachydactyly type A1 (BDA1) is part of the brachydactyly family of inherited disorders characterized by shortened phalanges or metacarpals. It was first identified by Farabee in 1903, and was the first recorded disorder of the autosomal dominant Mendelian trait in humans [31]. However, it was only recently that *IHH* was identified as a locus for BDA1 [17]. So far, heterozygous missense mutations in *IHH* have been identified in BDA1 patients [15, 16] and homozygous missense mutations in patients with Acrocapitofemoral Dysplasia [32].

The N-terminal fragment of Hedgehogs has all the known signaling activity, whereas the C-terminal fragment is responsible for the intracellular autoproteolytic processing during biosynthesis [33, 34]. Our assay of C3H10T1/2 cells for *Ptch1* and *Gli1* expression following induction with Wt IHH-N is consistent with the PTCH/SMO/GLI pathway. Here, we tested the signaling activities of the three *IHH* mutations (p.E95K, p.D100E and p.E131K) for BDA1 in cultured cells and demonstrated that these mutations do not result in a complete loss of function. However, the ability of the mutant IHHs to "fully" induce a Hedgehog response was significantly compromised when tested in C3H10T1/2 cells, suggesting similar outcomes in chondrocytes *in vivo*.

The three studied missense mutations (p.E95K, p.D100E p.E131K) all resulted in reduced Hedgehog signaling as determined by the reduced activation of the target genes *Ptch1* and *Gli1*. At the optimal induction concentration of 750 nM for unmodified Wt IHH-N proteins, *Gli1* induction was reduced by up to 80% for the mutant IHH-N proteins compared to the Wt, and no induction of *Ptch1* was detected from the mutant IHH-N proteins. It is not clear why there is a differential reduction between these two target genes. At this concentration, it is likely that for the Wt IHH-N proteins, the PTCH1 on the surface of the C3H10T1/2 cells is fully saturated with the HH proteins, while for the mutant IHH-N proteins, it is possible that there are still unbound PTCH1 receptors, and it is thus not possible to activate the signaling cascade to a level sufficient for *Ptch1* expression. This may be related to the proposed ratiomatric (the ratio between HH-bound and unbound PTCH1) activation of target genes [35].

The mechanism of how the missense mutations affect Hedgehog signaling is not fully understood. Given that they can transactivate some targets, albeit to a reduced level, they are not complete loss-of-function mutations, and some interaction with the receptor PTCH1 does occur. It is possible that the binding efficiency could be significantly affected. Because HH proteins can function across species, and vertebrate HH proteins activate a common pathway [6-9, 37], it is likely that the surface residues important for inductive activity and ligand/receptor interaction could be conserved. Indeed, the *IHH* mutations studied here are on conserved residues that could be involved in the binding with PTCH1 [17]. Although they are not at the exact position when aligned with the IHH-N protein sequence, similar engineered mutations (p.E90A, p.D132A and p.E138A) in the SHH-N proteins resulted in reduced binding coefficients for PTCH1 [36]. More recently, the p.E95K, p.D100E and p.E131K mutations were mapped on an X-ray crystal structure of SHH within a calcium binding site, a hotspot for mediating interactions with PTCH1, HIP1, CDO and GAS1 [18]. Furthermore, the p.D100E and p.E131K mutations were shown to affect IHH interaction with PTCH1 and HIP1 in a cell-based binding assay [18], and the effect of the p.E95K mutation was shown in a mouse model for BDA1, affecting binding to PTCH1 and HIP1, altering the capacity and range of signaling [19].

It is also possible that these mutations alter the interaction with the recently discovered PTCH1 binding partners, the *Ihog* surface proteins, CDO and BOC

[38-40], or the interaction with the cell surface HSPG such as glypican [41]. IHOGs and glypican cooperatively assist the binding of HH proteins to PTCH. This is important to fully activate the HH signaling. Interestingly, CDO is not expressed in C3H10T1/2 cells [42], so the observed reduced signaling potency is unlikely to be due to an altered interaction with CDO. The expressions of BOC in the C3H10T1/2 cells and CDO and BOC in the chondrocytes have yet to be determined, and would be important to test in the future to fully understand the molecular consequence of these mutations in IHH signaling.

Given that mice heterozygous for an *Ihh*-null allele have a normal skeletal and no observable digit abnormalities [19], and that *IHH* heterozygous mutations resulted in an abnormal digital phenotype in humans, the molecular mechanism for BDA1 is unlikely to be a simple reduction in the signaling potency of the mutant IHH proteins. Indeed, in the study of the mouse model for BDA1 [19], it was shown that a reduced signaling capacity may be responsible for a reduced growth of the long bones, and thus the associated short stature; however, there was also an extended range of signaling in the developing digits that may be the primary reason for the brachydactyly phenotype. While altered interaction with PTCH1 and HIP1 could in part explain the increased signaling range [19], it is possible that the BDA1 mutations could affect the formation of the multimeric complex, or interaction with HSPG, altering its diffusion through the matrix and thus the effective concentration gradient for short- and long-range signaling [26]. Furthermore, only limited targets of IHH signaling have been identified. Thus, to fully understand the molecular basis of the mutations and the consequences of an abnormal IHH signaling, it would be important to study additional genes that are altered as a consequence of the mutations.

To better understand the cascade of molecular signals that may be affected, we performed a microarray analysis by comparing the gene expression profiles from the activation of IHH signaling in the C3H10T1/2 cells. In the IHH activation of the mutant proteins, there were many genes that were either up- or down-regulated compared with the Wt (Tab. 2). Given that all three mutations result in BDA1, we considered the expression profiles of the three mutant proteins as biological replicates, and focused on the common genes that are down-regulated in all three mutant protein-activated cell lines, comparing them to the genes activated with the Wt IHH-N proteins.

There were five genes that satisfied these selection criteria, including the known target *Ptch1*. Of the four potential new targets, we confirmed the change in expression level for three genes, *Sostdc1*, *Penk1* and *Igfbp5*, via quantitative real-time PCR, with *Sostdc1* induced to the greatest extent upon IHH activation. These new targets were not significantly activated by the mutant IHH-N proteins. *Penk1* and *Igfbp5* were shown to be potentially regulated by GLI1, and their non-activation by the mutant IHH-N proteins is consistent with our observation that *Gli1* induction was impaired in mutant IHH-N-induced cells. The conserved 9-bp GLI1 binding motifs are present in the promoter regions of *Penk1* and *Igfbp5*, but absent in *Sostdc1*. Thus, *Sostdc1* appeared to be not

regulated through GLI1 from our finding, but is strongly up-regulated upon IHH signaling. Its expression has been implicated to be regulated by BMPs such as BMP2 and BMP7 [27].

The relationship between IHH and SOSTDC1 has not been previously demonstrated. However, SHH induction of digit elongation/extra phalanges is thought to be mediated by BMPs [43], linking HH and BMP signaling. Given that SOSTDC1 is a BMP antagonist [27], perhaps the regulation of BMP signaling by HH is via *Sostdc1* expression. Previous studies have shown that other BMP antagonists, such as NOGGIN and CHORDIN, are also up-regulated after *Ihh* misexpression in chicken [10], further substantiating a relationship between IHH and BMP signaling in skeletogenesis [44, 45].

Currently, several genes relating to brachydactylies have been identified, and these genes are related to BMP/TGFβ signaling. Mutations in *BMPR1B*, the high-affinity receptor for GDF5, cause brachydactyly type A2 (BDA2; OMIM 112600), a condition characterized by a shortening of the index finger due to hypoplasia/aplasia of the middle phalanx [46]. Overexpression of the mutant *BMPR1B* in the chick embryo resulted in a brachydactyly phenotype similar to that in humans; it acted in a dominant-negative manner [46]. Mutations in the human *GDF5* gene result in skeletal malformation syndromes including brachydactyly type C (BDC; OMIM 113100) [47]. The majority of mutations in *GDF5* described so far are nonsense and frame shift mutations that presumably result in a loss of function [48]. However, a recent study reported an R438L mutation in GDF5 that did not alter binding to BMPR1B but increased binding to BMPR1A, the receptor normally activated by BMP2, and this mutation resulted in the BDA2 phenotype [48]. Thus, altered BMP signaling as a result of impaired *SOSTDC1* expression due to abnormal IHH signaling for BDA1 is a possibility that needs to be tested.

The correlation of *PENK1* and *IGFBP5* to brachydactylies is less obvious. Insulin-like growth factor I (*IGF-I*) is expressed in the chondrocytes and has an essential role in endochondral ossification [49]. IGFBP5 is a member of a family of six high-affinity IGF-binding proteins that orchestrate IGF action, and is the most conserved of the IGFBPs between species [50]. Abnormal *Igfbp5* expression in mice results in whole-body growth inhibition and retarded muscle development [50]. A role in *in vitro* chondrogenesis has also been suggested [51], and *Igfbp5* was demonstrated to be regulated by SHH in early chicken embryogenesis [52]. *Igfbp5* is also found at higher levels in regions of cell death in the mouse mutant Hypodactyly, implying a role in limb bud development [53]. Our observed expression of *Igfbp5* in the mouse interdigital and phalangeal regions at E13.5 and E14.5 is consistent with a previous report [53]. However, we also showed expression in the interzone of the developing digit joints using two independent probes that we generated. This slight variation in the expression pattern may be related to the use of a mouse cDNA probe in the current study and a rat probe in the previous study [53].

Penk1 was first reported to modulate responses to painful stimuli [54]. At present, there is no information suggesting a link for *Penk1* to skeletogenesis. Its expression together with the *Igfbp5* in the *Gdf5* expression domain [55] of the developing joints is the first indication. In the *Ihh*-null mice, the lack of expression of these two genes in the developing digital joints further supports a link between IHH signaling and joint formation. However, it is possible that in the *Ihh*-null mice, the lack of *Penk1* expression in the presumptive joint regions is related to a developmental abnormality where the joints are not formed or delayed.

The roles of *Penk1* and *Igfbp5* in distal digit formation and how they may regulate joint development within the signaling network of IHH remains to be determined. Characterization of the potential digit and joint abnormalities in mouse mutants for these two genes, and studies of the genetic interactions with the BDA1 mouse [19] would provide further insights into the interactive network of genes and the brachydactyly phenotype.

REFERENCES

1. Nusslein-Volhard, C. and Wieschaus, E. Mutations affecting segment number and polarity in *Drosophila*. **Nature** 287 (1980) 795-801.
2. Levin, M., Johnson, R.L., Stern, C.D., Kuehn, M. and Tabin, C. A molecular pathway determining left-right asymmetry in chick embryogenesis. **Cell** 82 (1995) 803-814.
3. Riddle, R.D., Johnson, R.L., Laufer, E. and Tabin, C. Sonic Hedgehog mediates the polarizing activity of the ZPA. **Cell** 75 (1993) 1401-1416.
4. Echelard, Y., Epstein, D.J., St-Jacques, B., Shen, L., Mohler, J., McMahon, J.A. and McMahon, A.P. Sonic hedgehog, a member of a family of putative signaling molecules, is implicated in the regulation of CNS polarity. **Cell** 75 (1993) 1417-1430.
5. Bitgood, M.J., Shen, L. and McMahon, A.P. Sertoli cell signaling by Desert hedgehog regulates the male germline. **Curr. Biol.** 6 (1996) 298-304.
6. Vortkamp, A., Lee, K., Lanske, B., Segre, G.V., Kronenberg, H.M. and Tabin, C.J. Regulation of rate of cartilage differentiation by Indian hedgehog and PTH-related protein. **Science** 273 (1996) 613-622.
7. Chen, Y. and Struhl, G. Dual roles for patched in sequestering and transducing Hedgehog. **Cell** (1996) 87 553-563.
8. Marigo, V., Johnson, R.L., Vortkamp, A. and Tabin, C.J. Sonic hedgehog differentially regulates expression of GLI and GLI3 during limb development. **Dev. Biol.** 180 (1996) 273-283.
9. Lee, J., Platt, K.A., Censullo, P. and Ruiz i Altaba, A. Gli1 is a target of Sonic hedgehog that induces ventral neural tube development. **Development** 124 (1997) 2537-2552.
10. Pathi, S., Rutenberg, J.B., Johnson, R.L. and Vortkamp, A. Interaction of Ihh and BMP/Noggin signaling during cartilage differentiation. **Dev. Biol.** 209 (1999) 239-253.
11. Laufer, E., Nelson, C.E., Johnson, R.L., Morgan, B.A. and Tabin, C. Sonic hedgehog and Fgf-4 act through a signaling cascade and feedback loop to integrate growth and patterning of the developing limb bud. **Cell** 79 (1994) 993-1003.
12. Lanske, B., Karaplis, A.C., Lee, K., Luz, A., Vortkamp, A., Pirro, A., Karperien, M., Defize, L.H., Ho, C., Mulligan, R.C., Abou-Samra, A.B., Juppner, H., Segre, G.V. and Kronenberg, H.M. PTH/PTHrP receptor in early development and Indian hedgehog-regulated bone growth. **Science** 273 (1996) 663-666.
13. Bitgood, M.J. and McMahon, A.P. Hedgehog and Bmp genes are coexpressed at many diverse sites of cell-cell interaction in the mouse embryo. **Dev. Biol.** 172 (1995) 126-138.
14. St-Jacques, B., Hammerschmidt, M. and McMahon, A.P. Indian hedgehog signaling regulates proliferation and differentiation of chondrocytes and is essential for bone formation. **Genes Dev.** 13 (1999) 2072-2086.

15. Gao, B. and He, L. Answering a century old riddle: brachydactyly type A1. **Cell. Res.** <u>14</u> (2004) 179-187.
16. Byrnes, A.M., Racacho, L., Grimsey, A., Hudgins, L., Kwan, A.C., Sangalli, M., Kidd, A., Yaron, Y. and Lau, Y.L. Brachydactyly A-1 mutations restricted to the central region of the N-terminal active fragment of Indian Hedgehog. **Eur. J. Hum. Genet.** <u>17</u> (2009) 1112-1120.
17. Gao, B., Guo, J., She, C., Shu, A., Yang, M., Tan, Z., Yang, X., Guo, S., Feng, G. and He, L. Mutations in IHH, encoding Indian hedgehog, cause brachydactyly type A-1. **Nat. Genet.** <u>28</u> (2001) 386-388.
18. McLellan, J.S., Zheng, X., Hauk, G., Ghirlando, R., Beachy, P.A. and Leachy, D.J. The mode of Hedgehog binding to Ihog homologues is not conserved across different phyla. **Nature** <u>455</u> (2008) 979-983.
19. Gao, B., Hu, J., Stricker, S., Cheung, M., Ma, G., Law, K.F., Witte, F., Briscoe, J., Mundlos, S., He, L., Cheah, K.S. and Chan, D. A mutation in Ihh that causes digit abnormalities alters its signaling capacity and range. **Nature** <u>458</u> (2009) 1196-2000.
20. Hall, T.M., Porter, J.A., Beachy, P.A. and Leahy, D.J. A potential catalytic site revealed by the 1.7-A crystal structure of the amino-terminal signalling domain of Sonic hedgehog. **Nature** <u>378</u> (1995) 212-216.
21. Guo, S., Shi, Y., Zhao, X., Duan, S., Zhou, J., Meng, J., Yang, Y., Gu, N., Feng, G., Liu, H., Zhu, S. and He, L. No genetic association between polymorphisms in the AMPA receptor subunit GluR4 gene (GRIA4) and schizophrenia in the Chinese population. **Neurosci. Lett.** <u>369</u> (2004) 168-172.
22. Aoyama, S., Kase, H. and Borrelli, E. Rescue of locomotor impairment in dopamine D2 receptor-deficient mice by an adenosine A2A receptor antagonist. **J. Neurosci.** <u>20</u> (2000) 5848-5852.
23. Spinella-Jaegle, S., Rawadi, G., Kawai, S., Gallea, S., Faucheu, C., Mollat, P., Courtois, B., Bergaud, B., Ramez, V., Blanchet, A.M., Adelmant, G., Baron, R. and Roman-Roman, S. Sonic hedgehog increases the commitment of pluripotent mesenchymal cells into the osteoblastic lineage and abolishes adipocytic differentiation. **J. Cell. Sci.** <u>114</u> (2001) 2085-2094.
24. Nakamura, T., Aikawa, T., Iwamoto-Enomoto, M., Iwamoto, M., Higuchi, Y., Pacifici, M., Kinto, N., Yamaguchi, A., Noji, S., Kurisu, K. and Matsuya, T. Induction of osteogenic differentiation by hedgehog proteins. **Biochem. Biophys. Res. Commun.** <u>237</u> (1997) 465-469.
25. Pathi, S., Pagan-Westphal, S., Baker, D.P., Garber, E.A., Rayhorn, P., Bumcrot, D., Tabin, C.J., Blake Pepinsky, R. and Williams, K.P. Comparative biological responses to human Sonic, Indian, and Desert hedgehog. **Mech. Dev.** <u>106</u> (2001) 107-117.
26. Chen, M.H., Li, Y.J., Kawakami, T., Xu, S.M. and Chuang, P.T. Palmitoylation is required for the production of a soluble multimeric Hedgehog protein complex and long-range signaling in vertebrates. **Genes Dev.** <u>18 </u>(2004) 641-659.

27. Laurikkala, J., Kassai, Y., Pakkasjarvi, L., Thesleff, I. and Itoh, N. Identification of a secreted BMP antagonist, ectodin, integrating BMP, FGF, and SHH signals from the tooth enamel knot. **Dev. Biol.** 264 (2003) 91-105.

28. Walterhouse, D.O., Yoon, J.W. and Iannaccone, P.M. Developmental pathways: sonic hedgehog-patched-GLI. **Environ. Health Perspect.** 107 (1999) 167-171.

29. Yoon, J.W., Kita, Y., Frank, D.J., Majewski, R.R., Konicek, B.A., Nobrega, M.A., Jacob, H., Walterhouse, D. and Iannaccone, P. Gene expression profiling leads to identification of GLI1-binding elements in target genes and a role for multiple downstream pathways in GLI1-induced cell transformation. **J. Biol. Chem.** 277 (2002) 5548-5555.

30. Agren, M., Kogerman, P., Kleman, M.I., Wessling, M. and Toftgard, R. Expression of the PTCH1 tumor suppressor gene is regulated by alternative promoters and a single functional Gli-binding site. **Gene** 330 (2004) 101-114.

31. Farabee, W.C. hereditary and sexual influence in meristic variation: a study of digital malformations in man. Thesis, Harvard University, 1903.

32. Hellemans, J., Coucke, P.J., Giedion, A., De Paepe, A., Kramer, P., Beemer, F. and Mortier, G.R. Homozygous mutations in IHH cause acrocapito-femoral dysplasia, an autosomal recessive disorder with cone-shaped epiphyses in hands and hips. **Am. J. Hum. Genet.** 72 (2003) 1040-1046.

33. Lee, J.J., Ekker, S.C., von Kessler, D., Porter, J.A., Sun, B.I. and Beachy, P.A. Autoproteolysis in hedgehog protein biogenesis. **Science** 266 (1994) 1528-1537.

34. Porter, J.A., Ekker, S.C., Park, W.J., von Kessler, D.P., Young, K.E., Chen, C.H., Ma, Y., Woods, A.S., Cotter, R.J., Koonin, E.V. and Beachy, P.A. Hedgehog patterning activity: role of a lipophilic modification mediated by the carboxy-terminal autoprocessing domain. **Cell** 86 (1996) 21-34.

35. Casali, A. and Struhl, G. Reading the Hedgehog morphogen gradient by measuring the ratio of bound to unbound Patched protein. **Nature** 431 (2004) 76-80.

36. Fuse, N., Maiti, T., Wang, B., Porter, J.A., Hall, T.M., Leahy, D.J. and Beachy, P.A. Sonic hedgehog protein signals not as a hydrolytic enzyme but as an apparent ligand for patched. **Proc. Natl. Acad. Sci. U. S. A.** 96 (1999) 10992-10999.

37. Ekker, S.C., McGrew, L.L., Lai, C.J., Lee, J.J., von Kessler, D.P., Moon, R.T. and Beachy, P.A. Distinct expression and shared activities of members of the hedgehog gene family of *Xenopus laevis*. **Development** 121 (1995) 2337-2347.

38. Yao, S., Lum, L. and Beachy, P. The ihog cell-surface proteins bind Hedgehog and mediate pathway activation. **Cell** 125 (2006) 343-357.

39. Tenzen, T., Allen, B.L., Cole, F., Kang, J.S., Krauss, R.S. and McMahon, A.P. The cell surface membrane proteins Cdo and Boc are components and targets of the Hedgehog signaling pathway and feedback network in mice. **Dev. Cell.** 10 (2006) 647-656.

40. Zhang, W., Kang, J.S., Cole, F., Yi, M J. and Krauss, R.S. Cdo functions at multiple points in the Sonic Hedgehog pathway, and Cdo-deficient mice accurately model human holoprosencephaly. **Dev. Cell.** 10 (2006) 657-665.
41. Lin, X. Functions of heparan sulfate proteoglycans in cell signaling during development. **Development** 131 (2004) 6009-6021.
42. Kang, J.S., Mulieri, P.J., Miller, C., Sassoon, D.A. and Krauss, R.S. CDO, a robo-related cell surface protein that mediates myogenic differentiation. **J. Cell. Biol.** 143 (1998) 403-413.
43. Dahn, R.D. and Fallon, J.F. Interdigital regulation of digit identity and homeotic transformation by modulated BMP signaling. **Science** 289 (2000) 438-441.
44. Minina, E., Wenzel, H.M., Kreschel, C., Karp, S., Gaffield, W., McMahon, A.P. and Vortkamp, A. BMP and Ihh/PTHrP signaling interact to coordinate chondrocyte proliferation and differentiation. **Development** 128 (2001) 4523-4534.
45. Wu, Q., Zhang, Y. and Chen, Q. Indian Hedgeog is an essential component of mechanotransduction complex to stimulate chondrocyte proliferation. **J. Biol. Cem.** 276 (2001) 35290-35296.
46. Lehmann, K., Seemann, P., Stricker, S., Sammar, M., Meyer, B., Suring, K., Majewski, F., Tinscert, S., Grzeshcik, K. , Muller, D., Knaus, P., Nurnberg, P. and Mundlos, S. Mutations in bone morphogenetic protein receptor 1B cause brachydactyly type A2. **Proc. Natl. Acad. Sci. U. S. A.** 100 (2003) 12277-12282.
47. Polinkovsky, A., Robin, N., Thomas, J.T., Irons, M., Lynn, A., Goodman, F.R., Reardon, W., Kant, S.G., Brunner, G., van der Burgt, I., Chitayat, D., McGaugran, J., Donnai, D., Luyten, F.P. and Warman, M.L. Mutations in CDMP1cause autosomal dominant brachydactyly type C. **Nat. Genet.** 17 (1997) 18-19.
48. Seemann, P., Schwappacher, R., Kjaer, KW., Krakow, D., Lehmann, K., Dawson, K., Stricker, S., Pohl, J., Ploger, F., Staub, E., Nickel, J., Sebald, W., Knaus, P. and Mundlos, S. Activating and deactivating mutations in the receptor interaction site of GDF5 cause symphalangism or brachydactyly type A2. **J. Clin. Invest.** 115 (2005) 2373-2381.
49. Olney, R.C. and Mougey, E.B. Expression of the components of the insulin-like growth factor axis across the growth-plate. **Mol. Cell. Endocrinol.** 156 (1999) 63-71.
50. Salih, D.A., Tripathi, G., Holding, C., Szestak, T.A., Gonzalez, M.I., Carter, E.J., Cobb, L.J., Eisemann, J.E. and Pell, J.M. Insulin-like growth factor-binding protein 5 (Igfbp5) compromises survival, growth, muscle development, and fertility in mice. **Proc. Natl. Acad. Sci. U. S. A.** 101 (2004) 4314-4319.
51. Sekiya, I., Vuoristo, J.T., Larson, B.L. and Prockop, D.J. In vitro cartilage formation by human adult stem cells from bone marrow stroma defines the

sequence of cellular and molecular events during chon-drogenesis. **Proc. Natl. Acad. Sci. U. S. A.** 99 (2002) 4397-4402.

52. Allan, G.J., Zannoni, A., McKinnell, I., Otto, W.R., Holzenberger, M., Flint, D.J. and Patel, K. Major components of the insulin-like growth factor axis are expressed early in chicken embryogenesis, with IGF binding protein (IGFBP)-5 expression subject to regulation by Sonic hedgehog. **Anat. Embryol. (Berl)** 207 (2003) 73-84.

53. Allan, G.J., Flint, D.J., Darling, S.M., Geh, J. and Patel, K. Altered expression of insulin-like growth factor-1 and insulin like growth factor binding proteins-2 and 5 in the mouse mutant Hypodactyly (Hd) correlates with sites of apoptotic activity. **Anat. Embryol. (Berl)** 202 (2000) 1-11.

54. Konig, M., Zimmer, A.M., Steiner, H., Holmes, P.V., Crawley, J.N., Brownstein, M.J. and Zimmer, A. Pain responses, anxiety and aggression in mice deficient in pre-proenkephalin. **Nature** 383 (1996) 535-538.

55. Brunet, L.J., McMaon, J.A., McMaon, A.P. and Harland, R.M. Noggin, cartilage morphogenesis, and joint formation in the mammalian skeleton. **Science** 280 (1998) 1455-1457.